

TABLE OF CONTENTS

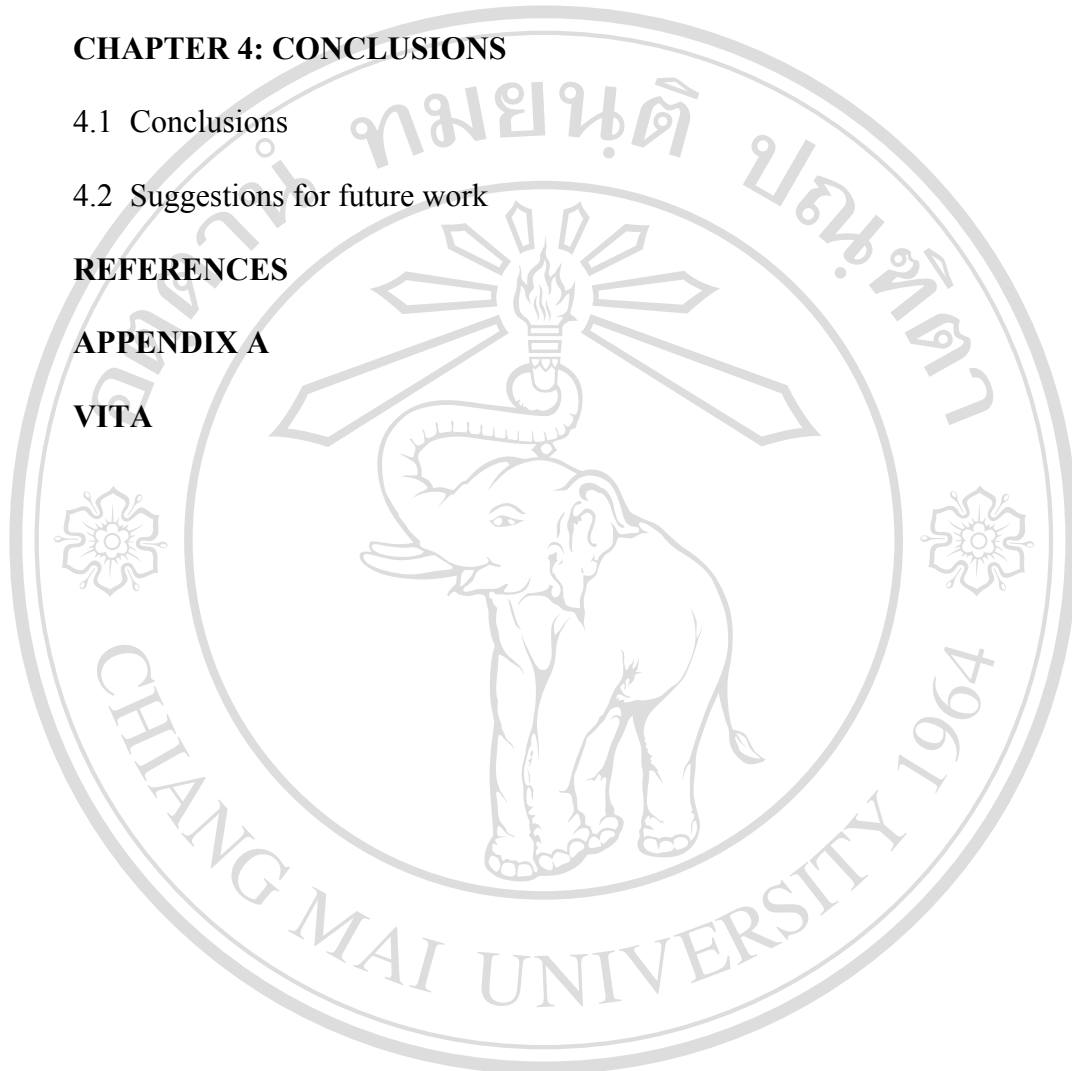
	Page
ACKNOWLEDGEMENT	iii
ABSTRACT (ENGLISH)	vi
ABSTRACT (THAI)	viii
LIST OF TABLES	xv
LIST OF ILLUSTRATIONS	xvi
ABBREVIATIONS AND SYMBOLS	xxii
 CHAPTER 1: INTRODUCTION	 1
1.1 Introduction	1
1.2 Bismuth sodium titanate	4
1.3 The ideal powder	9
1.3.1 Fine particle size	9
1.3.2 Unagglomerated particles	10
1.3.3 Narrow particle size distribution	10
1.4 Powder preparation	11
1.4.1 Mixed oxide reaction (conventional reaction)	12
1.4.2 Sol-gel method	13
1.4.3 Precipitation method	16
1.4.4 Hydrothermal method	19
1.4.4.1 Thermodynamic modeling	19

	Page
1.4.4.2 Standard-state properties for new solids	20
1.4.4.3 Stability and yield diagrams	24
1.4.4.4 Na-Bi-Ti-H ₂ O system	28
1.5 Objective of the work	31
CHAPTER 2: EXPERIMENTAL	32
2.1 Chemicals	33
2.2 Apparatus and instruments	33
2.3 Experimental procedures	34
2.3.1 Synthesis of BNT powders	34
2.3.1.1 Preparation of the solution	34
2.3.1.2 Hydrothermal process	34
2.3.2 Synthesis of BLNT powders	36
2.3.2.1 Hydrothermal process	36
2.4 Powders characterization	38
2.4.1 X-ray Diffraction (XRD)	38
2.4.2 Scanning Electron Microscopy (SEM)	38
2.4.3 Particle Size Distribution Analysis	39
2.5 Ceramics characterization	39
2.5.1 Ceramics preparation	39
2.5.2 X-ray Diffraction (XRD)	40
2.5.3 Scanning Electron Microscopy (SEM)	40
2.5.4 Measurement of density	40

	Page
CHAPTER 3: RESULTS AND DISCUSSION	42
3.1 Powders characterization	42
3.1.1 Crystalline structure determination	42
3.1.1.1 BNT powders from hydrothermal process	42
3.1.1.1.1 Effect of holding period at 200 °C	42
3.1.1.1.2 Effect of holding period at 150 °C	44
3.1.1.1.3 Effect of holding period at 175 °C	46
3.1.1.1.4 Effect of holding period at 200 °C	48
3.1.1.1.5 Effect of synthesis temperature and mineralizer concentration with holding period of 5 hours	50
3.1.1.1.6 Effect of synthesis temperature and mineralizer concentration with holding period of 15 hours	52
3.1.1.1.7 Effect of synthesis temperature and mineralizer concentration with holding period of 20 hours	54
3.1.1.2 BLNT powders from hydrothermal process	56
3.1.2 Microstructure analysis	60
3.1.2.1 BNT powders from hydrothermal process	60
3.1.2.1.1 Effect of holding period at 200 °C	60
3.1.2.1.2 Effect of holding period at 150 °C	62
3.1.2.1.3 Effect of holding period at 175 °C	64
3.1.2.1.4 Effect of holding period at 200 °C	66
3.1.2.2 BLNT powders from hydrothermal process	69

	Page
3.1.3 Particle size distribution analysis	72
3.1.3.1 BNT and BLNT powders from hydrothermal process	72
3.2 Ceramics characterization	76
3.2.1 Densification of BNT and BLNT ceramics	76
3.2.2 XRD patterns of BNT ceramics	79
3.2.3 Effect of sintering time on XRD patterns of BLNT ceramics with different mole %La	81
3.2.4 Effect of sintering time on XRD patterns of BLNT ceramics with different mole %La	83
3.2.5 Microstructure of BNT ceramics	85
3.2.6 Microstructure of BLNT ceramics sintered at 800 °C with different mole %La	88
3.2.7 Microstructure of BLNT ceramics sintered at 900 °C with different mole %La	90
3.2.8 Microstructure of BLNT ceramics sintered at 1000 °C for 2 hours with different mole %La	92
3.2.9 Microstructure of BLNT ceramics sintered at 1000 °C for 3 hours with different mole %La	94

	Page
CHAPTER 4: CONCLUSIONS	96
4.1 Conclusions	96
4.2 Suggestions for future work	99
REFERENCES	100
APPENDIX A	113
VITA	122



ลิขสิทธิ์มหาวิทยาลัยเชียงใหม่
 Copyright © by Chiang Mai University
 All rights reserved

LIST OF TABLES

Table	page
1.1 The lattice parameter of three structure phase transition of BNT	7
1.2 Standard state properties of solid species in the Na-Bi-Ti hydrothermal systems	24
1.3 Advanced oxide powder process comparison	30
3.1 The condition for hydrothermally synthesized of BNT and BLNT powders	58
3.2 Comparison the particle size of BNT powders from different process	68
3.3 Comparison the particle size of BLNT powders from different process	71
3.4 Comparison the particle size of BNT and BLNT powders from particle size distribution analysis	75
3.5 The measured density, % theoretical density, and % porosity of BNT and BLNT ceramics obtained from hydrothermal process	77
3.6 The comparison of the average grain size and theoretical density (%) of BNT ceramics from different processes	78
3.7 The comparison of average grain size and theoretical density (%) of BLNT ceramics from different processes	87

LIST OF ILLUSTRATIONS

Figure	Page
1.1 Basic structural unit of perovskite BNT	4
1.2 Octahedral framework with an A atom lie at the center of the unit cell	5
1.3 Phase diagram of $(\text{Na}_{1/2}\text{Bi}_{1/2})\text{TiO}_3\text{-PbTiO}_3$ near $(\text{Na}_{1/2}\text{Bi}_{1/2})\text{TiO}_3$	8
1.4 Solubility curves for various types of crystallization systems: curve A, isothermal solubility; curve B, positive temperature coefficient of solubility; curve C, negative temperature coefficient of solubility	17
1.5 Calculated stability and yield diagram in the Na-Bi-Ti- H_2O system at 200 °C as a function of solution pH. The symbols denote experimental conditions for which the following products were obtained: o, $\text{Bi}_4\text{Ti}_3\text{O}_{12} + \text{TiO}_2$; □, $\text{Bi}_4\text{Ti}_3\text{O}_{12} + \text{TiO}_2 + \text{Na}_{0.5}\text{Bi}_{0.5}\text{TiO}_3$; and ●, $\text{Na}_{0.5}\text{Bi}_{0.5}\text{TiO}_3$	25
1.6 Calculated stability and yield diagram in the Na-Bi-Ti- H_2O system at 200 °C as a function of NaOH concentration. The symbols denote experimental conditions for which the following products were obtained: o, $\text{Bi}_4\text{Ti}_3\text{O}_{12} + \text{TiO}_2$; □, $\text{Bi}_4\text{Ti}_3\text{O}_{12} + \text{TiO}_2 + \text{Na}_{0.5}\text{Bi}_{0.5}\text{TiO}_3$; and ●, $\text{Na}_{0.5}\text{Bi}_{0.5}\text{TiO}_3$	27
2.1 Schematic diagram for the preparation of BNT powders by hydrothermal process	36

Figure	Page
2.2 Schematic diagram for the preparation of BLNT powders by hydrothermal process	37
3.1 XRD patterns of BNT powders synthesized by hydrothermal process at 200 °C using 10 M NaOH as a mineralizer with different holding periods of (a) 5 h, (b) 10 h, (c) 15 h, and (d) 20 h	43
3.2 XRD patterns of BNT powders synthesized by hydrothermal process at 150 °C using 12 M NaOH as a mineralizer with different holding periods of (a) 5.45 h, (b) 10 h, (c) 15 h, (d) 20 h and (e) 25 h	44
3.3 XRD patterns of BNT powders synthesized by hydrothermal process at 175 °C using 12 M NaOH as a mineralizer with different holding periods of (a) 5 h, (b) 10 h, (c) 20 h, and (d) 30 h	46
3.4 XRD patterns of BNT powders synthesized by hydrothermal process at 200 °C using 12 M NaOH as a mineralizer with different holding periods of (a) 5 h, (b) 15 h, (c) 20 h, and (d) 45 h	48
3.5 XRD patterns of BNT powders synthesized by hydrothermal process with holding period of 5 h using 10-12 M NaOH as a mineralizer at different synthesis temperature (a) 10 M, 200 °C, (b) 12 M, 150 °C, (c) 12 M, 175 °C, and (d) 12 M, 200 °C	50
3.6 XRD patterns of BNT powders synthesized by hydrothermal process with holding period of 15 h using 10-12 M NaOH as a mineralizer at different synthesis temperature (a) 10 M, 200 °C, (b) 12 M, 150 °C, and (c) 12 M, 200 °C	52

Figure	Page
3.7 XRD patterns of BNT powders synthesized by hydrothermal process with holding period of 20 h using 10-12 M NaOH as a mineralizer at different synthesis temperature (a) 10 M, 200 °C, (b) 12 M, 150 °C, (c) 12 M, 175 °C, and (d) 12 M, 200 °C	54
3.8 XRD patterns of BLNT powders synthesized by hydrothermal process at 200 °C with holding period of 20 h using 12 M NaOH as a mineralizer and different mole %La of (a) 0 %La, (b) 1 %La, (c) 2 %La, (d) 3 %La, (e) 4 %La, (f) 5 %La and (g) 6 %La	57
3.9 SEM micrographs of BNT powders obtained from hydrothermal process at 200 °C using 10 M NaOH as a mineralizer with different holding periods of (a) 10 h, (b) 15 h, (c) 20 h, (d) 25 h, (e) 35 h and (f) 40h	61
3.10 SEM micrographs of BNT powders obtained from hydrothermal process at 150 °C using 12 M NaOH as a mineralizer with different holding periods of (a) 5.45 h, (b) 15 h and (c) 20 h	62
3.11 SEM micrographs of BNT powders obtained from hydrothermal process at 175 °C using 12 M NaOH as a mineralizer with different holding periods of (a) 5 h, (b) 10 h, (c) 25 h and (d) 30 h	64
3.12 SEM micrographs of BNT powders obtained from hydrothermal process at 200 °C using 12 M NaOH as a mineralizer with different holding periods of (a) 5 h, (b) 10 h, (c) 15 h, (d) 20 h, (e) 25 h (f) 40 h and (g) 60 h	66

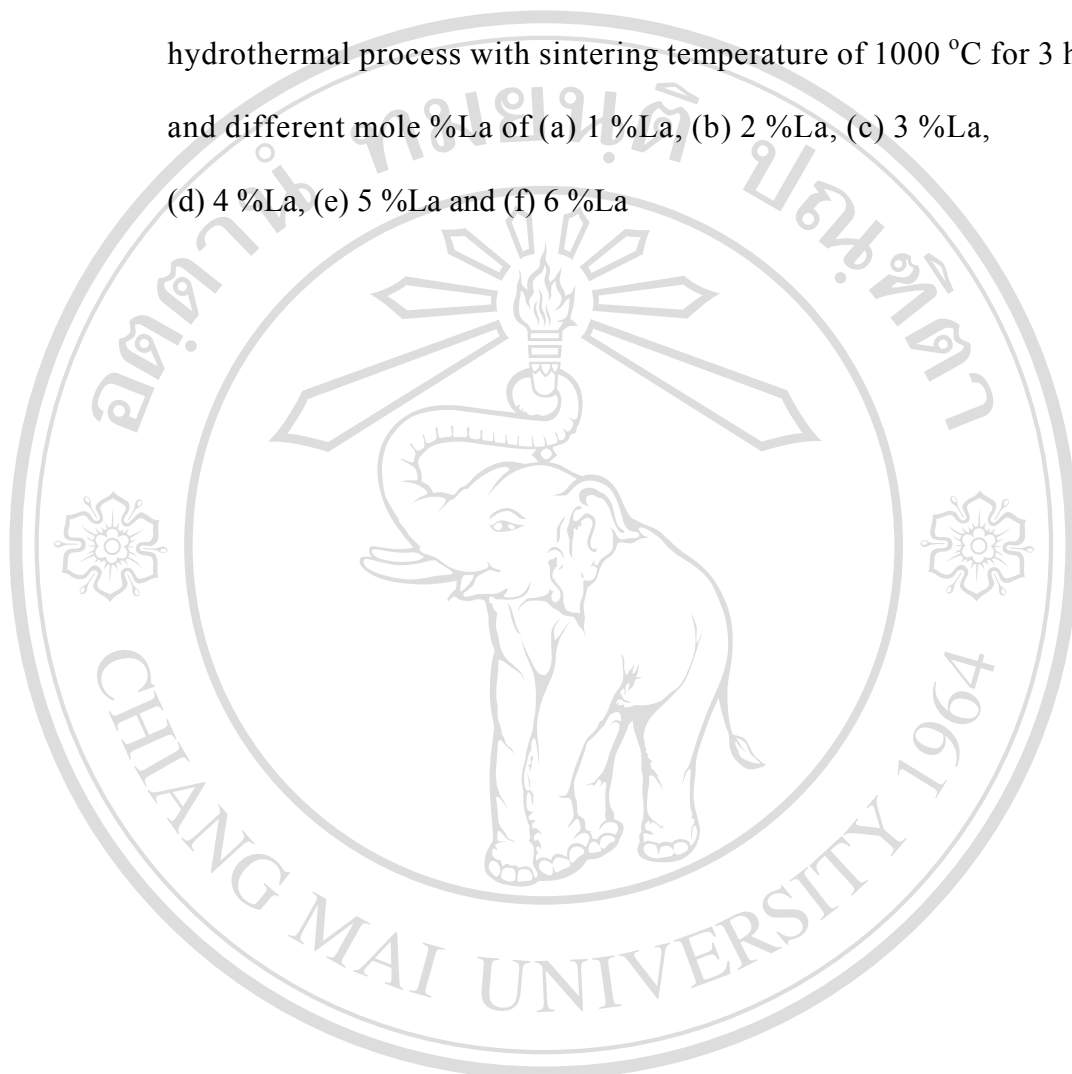
Figure	Page
3.13 SEM micrographs of BLNT powders obtained from hydrothermal process at 200 °C with holding period of 20 h using 12 M NaOH as a mineralizer and different mole %La of (a) 0 %La, (b) 1 %La, (c) 2 %La, (d) 3 %La, (e) 4 %La, (f) 5 %La and (g) 6 %La	70
3.14 Particle size distribution analysis of BLNT powders obtained from hydrothermal process at 200 °C with holding period of 20 h using 12 M NaOH as a mineralizer and different mole %La of (a) 0 %La, (b) 1 %La, (c) 2 %La, (d) 3 %La, (e) 4 %La, (f) 5 %La and (g) 6 %La	72
3.15 Particle size distribution analysis of BLNT powders obtained from hydrothermal process at 200 °C with holding period of 20 h using 12 M NaOH as a mineralizer and different mole %La of (a) 0 %La, (b) 1 %La, (c) 2 %La, (d) 3 %La, (e) 4 %La, (f) 5 %La and (g) 6 %La	73
3.16 XRD patterns of sintered BNT ceramics obtained from hydrothermal process sintered at 1000 °C for (a) 1 h, (b) 2 h and (c) 3 h	80
3.17 XRD patterns of sintered BLNT ceramics obtained from hydrothermal process sintered at 1000 °C for 2 h with different mole %La of (a) 0 %La, (b) 1 %La, (c) 2 %La, (d) 3 %La, (e) 4 %La, (f) 5 %La and (g) 6 %La	82

Figure	Page
3.18 XRD patterns of sintered BLNT ceramics obtained from hydrothermal process sintered at 1000 °C for 3 h with different mole %La of (a) 1 %La, (b) 2 %La, (c) 3 %La, (d) 4 %La and (e) 5 %La	84
3.19 SEM micrographs of BNT ceramics obtained from hydrothermal process at 200 °C using 12 M NaOH as a mineralizer with different sintering temperature and time of (a) 800 °C, 3 h, (b) 900 °C, 1 h, (c) 900 °C, 2 h, (d) 900 °C, 3 h, (e) 1000 °C, 1 h, (f) 1000 °C, 2 h and (g) 1000 °C, 3 h	86
3.20 SEM micrographs of sintered BLNT ceramics obtained from hydrothermal process with sintering temperature of 800 °C for 3 h and different mole %La of (a) 1 %La, (b) 2 %La, (c) 3 %La, (d) 4 %La, (e) 5 %La and (f) 6 %La	89
3.21 SEM micrographs of sintered BLNT ceramics obtained from hydrothermal process with sintering temperature of 900 °C for 3 h and different mole %La of (a) 1 %La, (b) 2 %La, (c) 3 %La, (d) 4 %La, (e) 5 %La and (f) 6 %La	91
3.22 SEM micrographs of sintered BLNT ceramics obtained from hydrothermal process with sintering temperature of 1000 °C for 2 h and different mole %La of (a) 1 %La, (b) 2 %La, (c) 3 %La, (d) 4 %La, (e) 5 %La and (f) 6 %La	93

Figure**Page**

- 3.23 SEM micrographs of sintered BLNT ceramics obtained from hydrothermal process with sintering temperature of 1000 °C for 3 h and different mole %La of (a) 1 %La, (b) 2 %La, (c) 3 %La, (d) 4 %La, (e) 5 %La and (f) 6 %La

95



ลิขสิทธิ์มหาวิทยาลัยเชียงใหม่
Copyright © by Chiang Mai University
All rights reserved

ABBREVIATIONS AND SYMBOLS

Å	Angstrom
AFE	Antiferroelectric
a.u.	Arbitrary Unit
Bi	Bismuth
BLNT	Bismuth lanthanum sodium titanate
BNT	Bismuth sodium titanate
C_{eq}	Solubility
C_p	Heat Capacity
°C	Degree Celcius
FE	Ferroelectric
h	Hours
JCPDS	Joint Committee for Powder Diffraction Standards
kV	Kilovoltage
K_p	Electromechanical Coupling Coefficient
La	Lanthanum
M	Molar
mA	Milliampere
min	minute
mm	Millimeter
Mpa	Magapascal
MPB	Morphotropic Phase Boundary
nm	Nanometer

nm^3	Volume nanometer
O	Oxygen
PE	Paraelectric
PLZT	Lead Lanthanum Zirconate Titanate
PMN	Lead Magnesium Niobate
S°	Absolute Entropy at a Reference Temperature
SEM	Scanning Electron Microscope
T	Temperature
T_c	Curie Temperature
Ti	Titanium
V°	Partial molar Volume
XRD	X-ray Diffraction
ϵ_{max}	Maximum of dielectric permittivity
ϵ_r	Dielectric Constant
ΔG_f°	Standard Gibbs Energy
ΔH_f°	Enthalpy of Formation
μm	Micrometer
%	Percentage